

Prediction of fatigue life of aluminum 2024-T3 at low temperature by finite element analysis

S. Mazlan¹, N. Yidris^{1*}, R. Zahari², E. Gires¹, D.L.A Majid¹ and K.A. Ahmad¹

¹ Department of Aerospace Engineering, Universiti Putra Malaysia, 43400 UPM Serdang, Selangor, Malaysia

Tel: +603 - 9769 4413; Fax: +603 - 9769 4488

² System Engineering Department, Military Technological College, P.O Box 262 PC 111, Muscat, Sultanate of Oman

ABSTRACT – The change in material properties at low temperature has always been one of the concerned design factors in aircraft industries. The wings and fuselage are repeatedly exposed to sub zero temperature during cruising at high altitude. In this study, fatigue tests were conducted on standard flat specimens of aluminum 2024-T3 at room temperature and at -30 °C. The monotonic and cyclic loading tests were conducted using MTS 810 servo hydraulic machine equipped with a cooling chamber. The monotonic tests were conducted at a crosshead speed rate of 1 mm/min and the cyclic tests at a frequency of 10 Hz with a load ratio of 0.1. The experimental data obtained, such as the yield strength, ultimate strength and S-N curve were used as the input parameters in ANSYS Workbench 16.1. This close agreement demonstrates that the isotropic model in ANSYS workbench is essential in predicting fatigue life. The increase in stress parameter causes fatigue life to decrease. Besides, the decrease in temperature causes the total fatigue life to increase.

ARTICLE HISTORY

Revised: 26th Apr 2020

Accepted: 07th Sep 2020

KEYWORDS

Aluminum 2024-T3;
fatigue test;
room temperature;
low temperature;
ANSYS workbench

INTRODUCTION

Aluminum alloy has been broadly used in automotive and aircraft industries because it has a high elastic modulus, high strength and low density [1, 2]. The fuselage, wings and lightweight parts are usually designed using this material. Some of the structures are not required to have infinite fatigue life [3]. However, the design must be able to meet the expected, desired fatigue life and safety of the components.

Typically the airframe of an aircraft is an example of the structures prone to fatigue. Stresses that occurred repeatedly due to frequency and flight cycles weaken the structures. After a particular amount of time, a microscopic crack will initiate from the weakest area and the visibility increases as it propagates. The pressure from turning, decelerating and accelerating also contributes to the crack propagation rate. The cross-sectional area decreases when exposed to repeated loading that leads to fractures causing the structure to fail. The influence of the environment, type of material and level of stress will impact the fracture mode of the structure [4].

Some researches have been carried out to study the fatigue life of aluminum alloy at low cycles ($LCF < 10^4$) and high cycles ($HCF < 10^7$) [5–8]. Besides, additional life cycles can be categorized as a very high cycle (VHCF) fatigue. The reason why the low cycle fatigue is important is due to the highly repeated loading in certain parts of aircraft such as fuselage, wings and turbine engines. However, to run experimental testing in order to obtain the S-N curve for each structure is time consuming and expensive. Numerical simulation can be applied to the problem to predict the fatigue life. This approach enables users to know the strength and weakness of the design and make further improvements in advanced.

The components of aircraft structures are always exposed to low temperature during ascending. The temperature in that situation can be as low as -50°C. During the mid-1970s, researchers started to notice the behavior of aluminum under fatigue loading at low temperature, which several studies reported the decreasing in fatigue crack growth rate and toughness [9–11] as the effects. A similar study also concluded that Fatigue Ductile-Brittle Transition (FDBT) occurred due to the decreasing of crack growth rate and starts to increase until failure at low temperature [12]. Furthermore, the fatigue and tensile strength increase even at a cooling rate 1 °C per minute in cooling chamber [13] causes decrease in grain size and increasing in particle density [14]. The prediction of the fatigue life does not only rely on the engineering problem alone, but also the condition of the material as well. Scratches and unpolished surfaces contribute to crack initiation that starts from micro to macro scale [15]. Several fatigue models were investigated under different cyclic loading and found that the best model is based on experience related to the problem [16].

The use of finite element analysis (FEA) can be one of the unconventional ways of predicting fatigue life. This numerical method is able to answer the problem, not only related to structural but fluid, thermal and electrical. Moreover, with the use of numerical analysis software, the strength and weakness of the model known in advance which able the user to make some improvements. There are varieties of numerical software available such as SolidWorks, ABAQUS, MSC NASTRAN and ANSYS Workbench. The focus will be more on ANSYS Workbench for predicting fatigue life as there are limited studies related to this area. Numerous numbers of studies [17–22] reported by researchers in predicting fatigue life theoretically or by comparing with experimental results. Surprisingly, they preferred using alternative

Computer Aided Design (CAD) software for 3D modeling and imported the file to ANSYS Workbench for analysis. Even though the software has its own workspace for modeling, the experience for ideal CAD software reduces the time taken in the design.

In the real world situation, it is not possible to alter the properties of the material. The numerical or analytical approach is more suitable in predicting different results. The effect of isotropic hardening on fatigue crack growth causes the rate to decrease when the hardening parameter increases [23]. Moreover, similar case with kinematic hardening shows that the crack growth was longer compared to isotropic hardening [24]. Still, combined hardening successfully predicts cycles to fail in the case of ultra-low cycle fatigue pipeline simulation [25]. A study on low cycle fatigue of 304 LN stainless steel by cyclic hardening displays the importance of the level of loading [26]. The fatigue of aluminum 2024-T3 is focusing on isotropic hardening under uniaxial loading with low plasticity that fits the suitability of the software in predicting closer results to experimental.

The aim of this study is to predict the life cycles of aluminum 2024-T3 using the numerical software, ANSYS Workbench at room and low temperature. The monotonic tensile test and cyclic test with several levels of loading were performed in order to obtain the mechanical properties and fatigue life data which be used as the input to the software. The results are then compared to show the efficiency.

METHODOLOGY

Experimental Procedures

The selected test material is aluminum 2024-T3 which has been used in the main aircraft components due to its excellent fatigue strength and high toughness. A plate of aluminum with dimension of 200 mm x 20 mm x 3 mm was cut following the ASTM E8M standard [27]. The chemical composition is presented in Table 1. The monotonic tensile test and cyclic test were run in two conditions, at room and low temperature. The grips of the machine were aligned and the grip pressure of 700 psi was selected for the specimens. The tension tests at room temperature were performed using MTS 810 servo hydraulic testing machine as shown in Figure 1(a) at a displacement rate of 1 mm/min to obtain the mechanical properties such as the yield strength and ultimate strength.

Table 1. Chemical composition of aluminum 2024-T3 [28]

Element	Wt%
Fe	0.28
Mn	0.43
Cu	4.4
Si	0.14
B	0.003
Zn	0.12
V	0.02
Mg	1.4
Al	Balance



Figure 1. MTS 810 servo hydraulic machine set up at: (a) room temperature and (b) low temperature

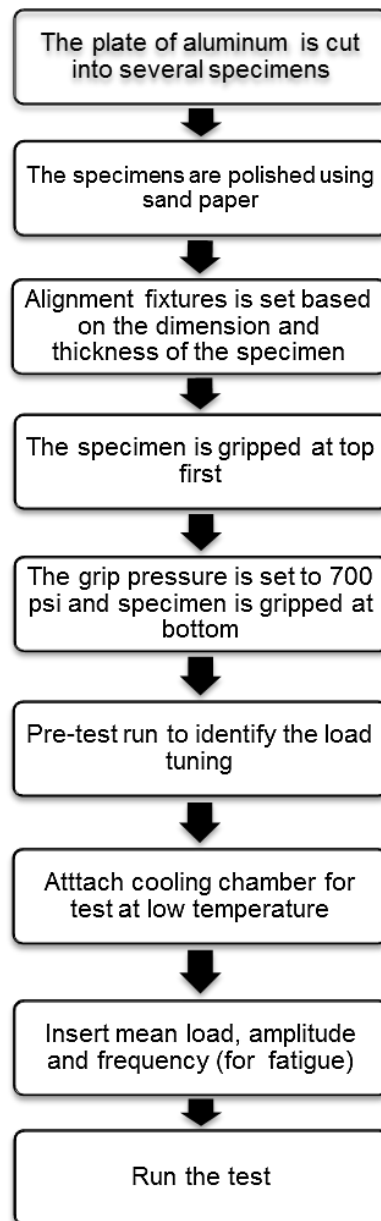


Figure 2. A diagram representing steps for running test using MTS 810

The steps to run test using MTS 810 is shown in Figure 2. At low temperature, the MTS 810 machine was equipped with a cooling chamber with minimum temperature of $-40\text{ }^{\circ}\text{C}$ as shown in Figure 1(b). The tensile tests were carried out at temperature $-30\text{ }^{\circ}\text{C}$. The temperature was measured using K type thermocouples connected to the digital thermometer TM902C. The thermocouples were placed at four different places as shown in Figure 3. The tests at low temperature were performed after reaching the preferred temperature at a displacement rate of 1 mm/min to acquire the mechanical properties.

The cyclic tests at room and low temperature were conducted according to the ASTM E466 standard [29] with a frequency of 10 Hz in sinusoidal waveform and a load ratio of 0.1 to obtain the S-N curve of the material. The loading starts at 90% of the yield strength as shown in Table 2, decreasing by 5% to 70% of yield. In addition, the values of the mean and amplitude load were also taken based on the percentage of the yield strength.

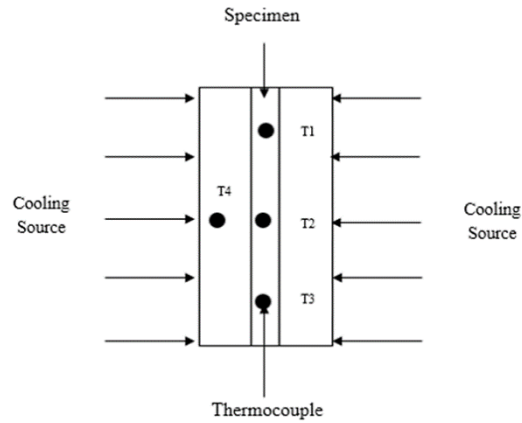


Figure 3. Location of thermocouple inside cooling chamber

The following equations are used to calculate the values needed as input for the MTS 810 testing machine [30]:

$$R = \frac{S_{min}}{S_{max}} \quad (1)$$

where in Eq. (1), R is the load ratio, S_{min} is the minimum stress and S_{max} is the maximum stress. The difference between maximum and minimum stress can be calculated by using Eq. (2), stress range, σ_R :

$$\sigma_R = S_{max} - S_{min} \quad (2)$$

To plot the S-N curve the value of alternating stress, σ_a is often used. This is given by Eq. (3):

$$\sigma_a = \frac{S_{max} - S_{min}}{2} \quad (3)$$

The mean stress σ_m is important in the prediction of fatigue life can be given as Eq. (4):

$$\sigma_m = \frac{S_{max} + S_{min}}{2} \quad (4)$$

Numerical Procedures

The specimen was modeled in SolidWorks 2012 with dimension of 200 mm x 20 mm x 3 mm as shown in Figure 4. Before the sketch was drawn, a top plane feature was first selected. The boss extrude feature was selected to generate the 3D model with 3 mm thickness. Next, the 3D model saved in an IGES format exported to ANSYS Workbench as shown in Figure 6(a).

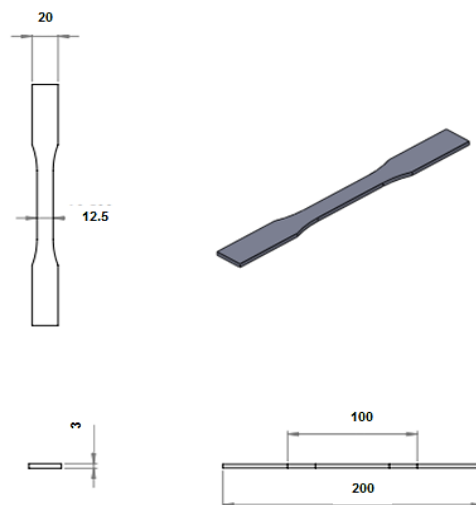


Figure 4. Dimension of specimen (mm)

The static structural analysis system was selected to simulate the fatigue life, maximum stress and alternating stress of the model. A coarse mesh was selected with SOLID187 hexahedrons as shown in Figure 6(b), which is a 10-node element suitable for 3D model imported from other CAD software. The size of the mesh also influences the accuracy of the results. As the mesh becomes finer, the computation time increases. The mesh convergence of the model is run as shown in Figure 5 to obtain the experimental results as close as possible with low computational time. There is a great increase in the number of nodes from 431 to 1573 and the number of elements from 44 to 759.

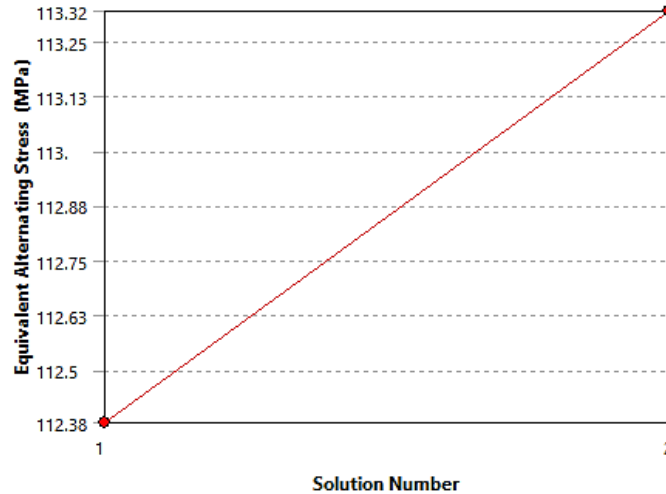


Figure 5. Mesh convergence plot for the 3D model

Furthermore, similar boundary condition from experimental setup was applied to the 3D model. As from Figure 6 (c), A indicates all degrees of freedom fixed and B points out the load direction. At fatigue tool options, stress-life was selected as the type of analysis with load ratio 0.1. The stress life analysis in ANSYS uses the interpolation method to the S-N curve of experimental data to find a suitable value. The yield strength, ultimate strength, mean stress, alternating stress and S-N curve obtained from experimental tests were used as an input to the software.

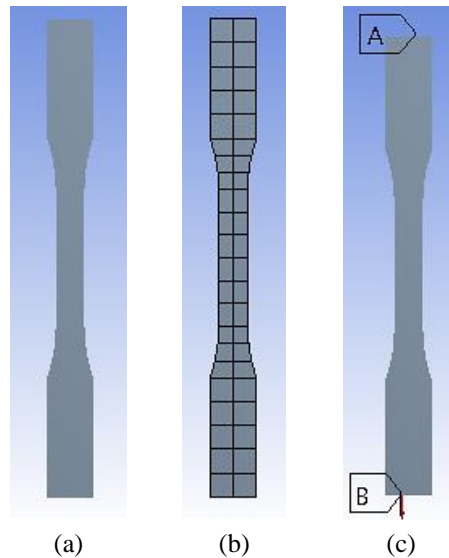


Figure 6. (a) The imported 3D model, (b) meshed 3D model and (c) applied boundary condition of the model

RESULTS AND DISCUSSION

Fatigue Surface Failure

The initiation of crack at flat specimen during a tensile test is due to the concentration of damage and deformation in the area leading to shear rupture. The mechanical properties of aluminum obtained from tension test are presented in Table 2. For low temperature condition, there is an increase of 10.70% in the yield strength and 3.90% in the ultimate strength compared to room temperature.

Table 2. Mechanical properties of aluminum 2024-T3 from tension test

Condition	Yield strength (MPa)	Ultimate strength (MPa)
Room temperature	327	487
Low temperature	362	506

The formation of micro crack occurred at stress concentration area of the specimen after subjected to cyclic loading for a period of time. The crack initiation is noticeably caused from the surface of the material [31]. The crack then propagates perpendicular to the loading until the critical length is reached before failure occurs. The visibilities of fracture surfaces, shiny, and smooth area with the muddled wavy appearance [32] can be witnessed in Figure 7.

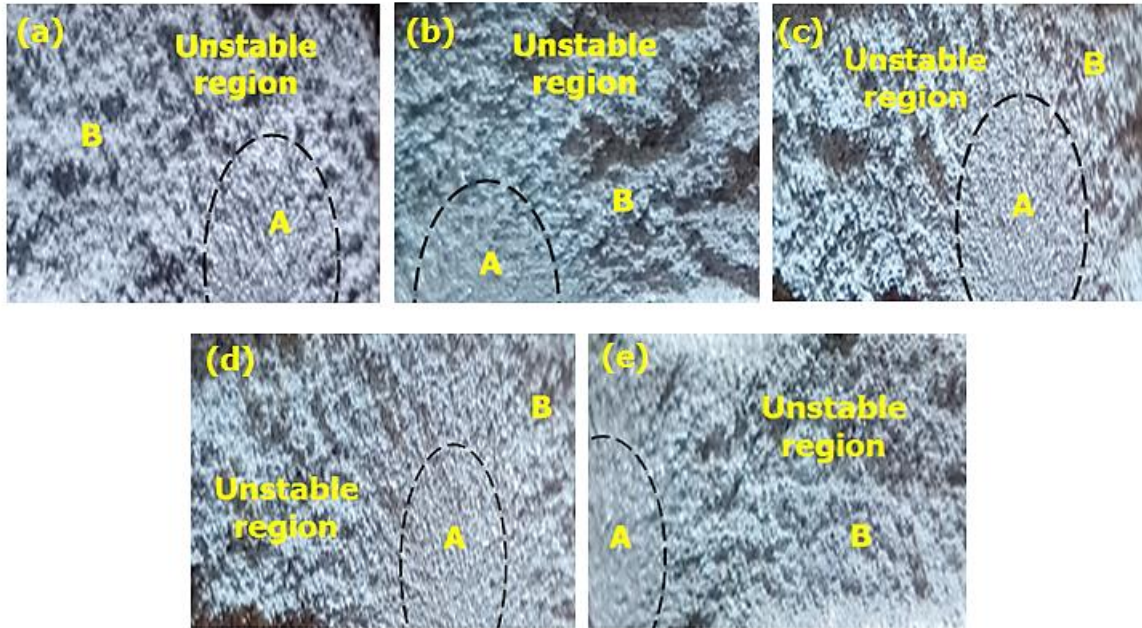
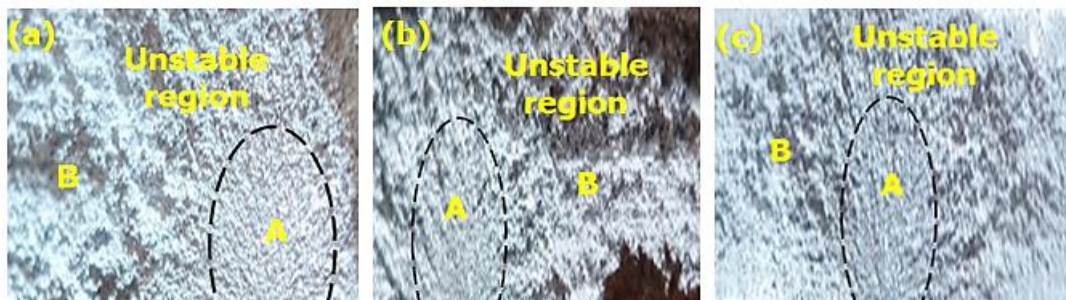


Figure 7. Surface crack some of the specimens at room temperature: (a) 90%, (b) 85%, (c) 80%, (d) 75% and (e) 70%

The fracture surface areas are separated into two regions, stable and unstable crack growth. Area A represents the stable region and area B represents unstable region. Besides, the circle in Figure 7 indicates the stable crack region that has small dimple structure and the unstable crack region has bigger dimple structures [28]. In addition, the direction of loading causes perpendicular stable crack grows and unloading causes unstable crack growth. The crack region with stable growth is smaller at high level loading compared to low loading.

One of the reasons in increasing yield strength and ultimate strength of aluminum at low temperature is decreasing of the grain size when tested at low temperature. For this reason, the density of the particles also increases. The effect of cyclic loading of the material after a certain amount of time leads to the formation of micro cracks at stress concentration area. The grain size, surfaces and slip bands are factors that contribute to crack initiation. Moreover, the failure can occur even with small plastic deformation of ductile materials.



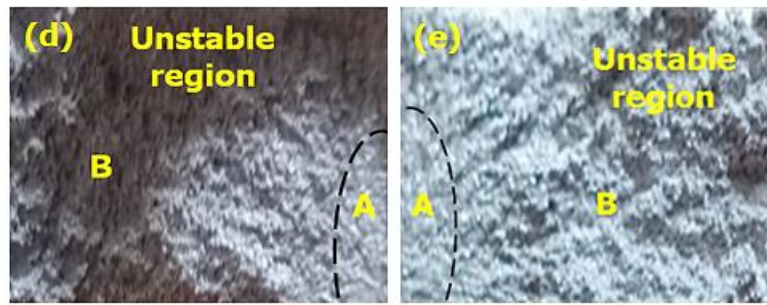


Figure 8. Fatigue surface failure of the specimens at low temperature: (a) 90%, (b) 85%, (c) 80%, (d) 75% and (e) 70%

Figure 8 represents the surface failure of the material from 90% to 70% of the yield strength. The small circle, A indicated the area where crack initiation starts and propagates until area B before failure occurred. The micro crack grows in stable rate to macro crack until failure [33]. Moreover, at higher loading the crack reaches the critical length faster, which causes rapid fracture.

However, at low temperature the crack growth rate and fracture toughness decreases. This can be observed clearly at 70% and 75% of the yield strength as the crack growth areas were small compared to others. Mode I failure was observed at all surfaces since uniaxial loading was applied to the specimens. The visibility of shear lips can be seen around the crack propagation area B.

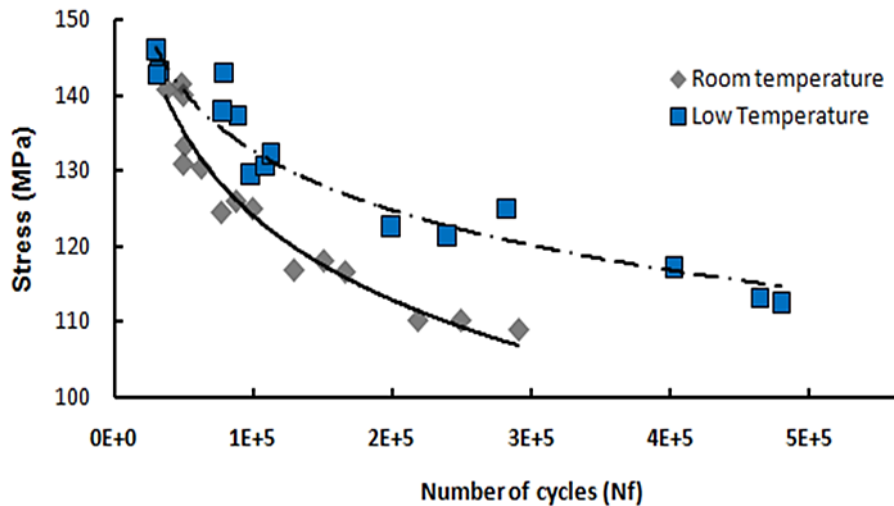


Figure 9. S-N curve at room and low temperature of aluminum

The trend lines for stress (MPa) against the number of cycles (N_f) under load ratio 0.1 are shown in Figure 9. It can be witnessed that the number of cycles, increased as stress decreased for both lines. The line consists of results obtained at room and low temperature starting from 90% to 70% of the yield strength. There is an increase of 18.90% in the number of cycles from 90% to 85%. At higher loads the damage nucleated faster causes fatigue life to be lower. Meanwhile, there was a constant increase in the number of cycles from 80%, 75% and 70% that are 63.62%, 68.66% and 69.93% respectively.

Nevertheless, there is a decrease of 30.31% for a number of cycles at 90% of the yield strength at low temperature compared to room temperature. The exposure to low temperature decreases the crack growth rate that causes sudden failure at high loading due to the material entering from ductile to brittle state. The equation to calculate the fatigue life can be described as:

$$\sigma_a = m \ln(N_f) + C \quad (5)$$

The value of m and C are obtained from the experimental data. The value for m and C at room temperature is 16.1 and 310.1 respectively. While at low temperature the value of $m=11.5$ and $C=265.7$. The highest increase in the number of cycles at low temperature compared to room temperature can be observed clearly at 70% and 75% with an increase of 77.58% and 62.05%. When the material subjected to the lower percentage of loading and low temperature for a certain period of time, the particle density and grain size decrease causes slower crack growth rate and increase in number of cycles.

Numerical Results

The application of ANSYS to predict the fatigue life is proven by validating the results with other researcher's work. The study by Pereira et al. (2018) upon the fatigue behavior of Inconel 625 at room temperature is taken as a comparison with ANSYS. The material has a yield strength of 472 MPa and an ultimate strength of 935 MPa. The loading starts from 125%, 100%, 81% and 65% of the yield strength [34]. The constant amplitude ratio of $R = -1$ and frequency of 10 Hz was applied during fatigue testing of the Inconel 625 specimens.

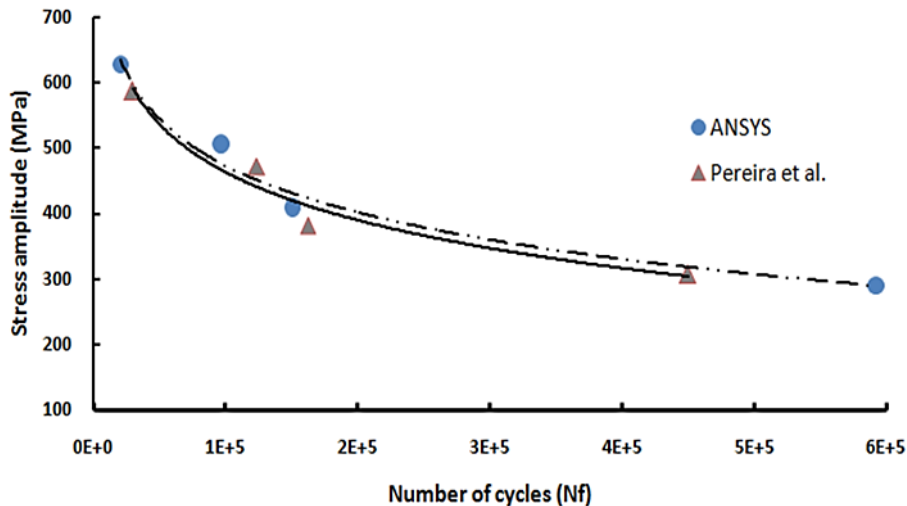


Figure 10. Comparison of ANSYS results with Pereira et al. (2018)

The S-N curve in Figure 10 shows the comparison of results from ANSYS and Pereira et al. (2018). The fatigue life decreases as the stress increases. At 125% of loading, the stress amplitude of ANSYS shows 627.14 MPa and Pereira 586 MPa respectively. Around 6.56% difference is obtained between the stresses. As a result, ANSYS predicted lower fatigue life due to higher stress, at 20978 cycles and Pereira at 30000 cycles that estimated about 30% differences.

Similarly, the difference in stress at 100% of loading is 6.56%. Still, the difference in fatigue life is lower, around 22%. Besides, at 61% of loading the stress and fatigue life has the same percentage of difference that is about 7%. However, at 65% of loading, ANSYS predicted lower stress than Pereira about a 5.58% difference. The difference causes fatigue life predicted by ANSYS to increase by 25% compared to the Pereira result. The overall results show an excellent agreement between ANSYS along with another researcher and can be used for the life prediction of aluminum 2024-T3.

The fatigue life at room temperature for aluminum 2024-T3 is plotted in Figure 11. Two S-N curves represent the experimental and the simulation results. An increase in stress will have corresponding decrease in the fatigue life. The low cycle fatigue ranges from 90% to 80% and the high cycle fatigue from 75% to 70% of the yield strength. At 90%, ANSYS predicted stress, greater than the experimental results by 4%. The fatigue life with regard to ANSYS is 42692 cycles and experimental 45343 cycles. There is about 5.8% difference between the two scenarios.

Moreover, the stress at 85% of experimental is lowered by 5% compared to ANSYS resulting 10% higher for the fatigue life. The percentage of difference at 80% increase by 21.5% for experimental compared to ANSYS although there is only 4% difference in stress. Besides, ANSYS predicted lower fatigue life compared to experimental by 22.4% at 75% of the yield strength. Also, there is only 3.5% difference in stress at 70% of the yield strength and 20% increase in experimental compared to simulation.

The comparison of S-N curves of aluminum 2024-T3 at low temperature is shown in Figure 12. The fatigue life of aluminum is validated by simulation and experimental. The decrease in stress increases fatigue life. The stress at 90% of the yield strength of experimental is 144.06 MPa and simulation 151.29 MPa that shows about 4.8% difference. Since the experimental stress is lower, the fatigue life is higher by 25% compared to simulation. Besides, the fatigue life at 85% of the yield strength displays 82133 cycles for experimental and 59819 cycles for simulation. The difference is about 27%, even though the difference between stresses is only 2.4%. The fatigue life at 80% of the yield strength illustrates 106830 cycles for experimental and 96555 cycles for the simulation that indicates a 9.6% difference. There is around 2.8% difference for the stress. In addition, there is a 2.5% difference in stress and a 22% difference in fatigue life at 75% of the yield strength. Also, the fatigue life at 70% shows a difference of 17% and approximately 3% of the stress difference.

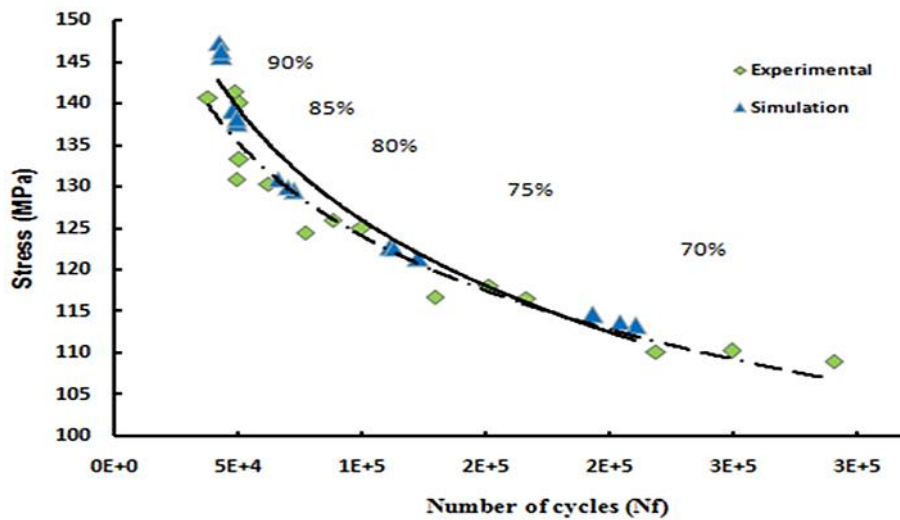


Figure 11. Comparison of results between experimental and ANSYS at room temperature

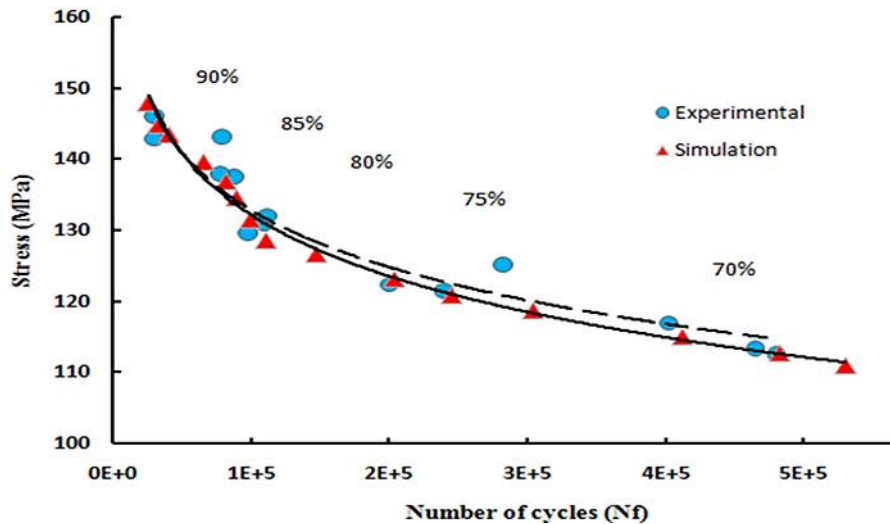


Figure 12. Comparison of results between experimental and ANSYS at low temperature

The grain shapes, sizes and orientations strongly influence the properties of the material when exposed to a certain temperature. The common crack initiation for aluminum is due to material inhomogeneities. Some specimens may have unpolished or scratch surfaces including micropores and constituent particles [35, 36]. In addition, for ANSYS the prediction is based on applied stress. Lower stresses will result, a higher number of cycles. A close trend can be observed for both scenarios, which proved a good agreement.

CONCLUSION

The cyclic tests of aluminum 2024-T3 were investigated at room and low temperature at load ratio of 0.1 and frequency of 10 Hz. The effect of low temperature on aluminum caused an increase in yield strength, ultimate strength and fatigue life. This is due to the decreasing in crack growth rate, which at the same time decreases the grain size and increases the particle density. Separation of two regions, stable and unstable crack growth was clearly observed in the fracture surface area. The simulation of predicting fatigue life was conducted using ANSYS Workbench. It is found that at room temperature for the low cycle fatigue the variance between stresses range from 4%-5%. The difference between the high cycles is around 3.5% to 4.2%. The lowest fatigue life difference is 5.8% at 90% and the highest is 22.4% at 75%. Furthermore, at low temperature, a maximum difference of 4.8% in stress is observed between experimental and simulation. A minimum difference of 2.4% is seen at 75% of the yield strength. The fatigue life shows a maximum and minimum difference of 27% and 9.6% respectively. The trend line of the S-N curve in ANSYS successfully predicted results close to experimental data.

ACKNOWLEDGMENT

This research was funded by the Ministry of Higher Education of Malaysia, grant number FRGS/1/2015/TK09/UPM/02/1.

REFERENCES

- [1] A. Heinz, A. Haszler, C. Keidel, S. Moldenhauer, R. Benedictus, and W. S. Miller, "Recent development in aluminium alloys for aerospace applications," *Mater. Sci. Eng. A*, vol. 280, no. 1, pp. 102–107, 2000, doi: [https://doi.org/10.1016/S0921-5093\(99\)00674-7](https://doi.org/10.1016/S0921-5093(99)00674-7).
- [2] T. Dursun and C. Soutis, "Recent developments in advanced aircraft aluminium alloys," *Mater. Des.*, vol. 56, pp. 862–871, 2014, doi: <https://doi.org/10.1016/j.matdes.2013.12.002>.
- [3] S. Saleem Khan, D. Hellmann, O. Kintzel, and J. Mosler, "An experimental and numerical lifetime assessment of Al 2024 sheet," *Procedia Eng.*, vol. 2, no. 1, pp. 1141–1144, 2010, doi: <https://doi.org/10.1016/j.proeng.2010.03.123>.
- [4] X. Jin, "Key problems faced in high-speed train operation," *J. Zhejiang Univ. Sci. A*, vol. 15, pp. 936–945, 2014.
- [5] K. Hockauf, M. F.-X. Wagner, T. Halle, T. Niendorf, M. Hockauf, and T. Lampke, "Influence of precipitates on low-cycle fatigue and crack growth behavior in an ultrafine-grained aluminum alloy," *Acta Mater.*, vol. 80, pp. 250–263, 2014, doi: <https://doi.org/10.1016/j.actamat.2014.07.061>.
- [6] M. Delbove, J. B. Vogt, J. Bouquerel, T. Soreau, N. François, and F. Primaux, "Microstructure Evolution of a Precipitation Hardened Cu-Ni-Si Alloy during Low Cycle Fatigue," in *Materials Structure & Micromechanics of Fracture VIII*, 2017, vol. 258, pp. 546–549, doi: 10.4028/www.scientific.net/SSP.258.546.
- [7] W. Ziája, M. Motyka, H. Dybiec, and J. Sieniawski, "High cycle bending fatigue life of submicrocrystalline aluminum alloy," *Mech. Mater.*, vol. 67, pp. 33–37, 2013, doi: <https://doi.org/10.1016/j.mechmat.2013.07.013>.
- [8] Y. Takahashi, T. Shikama, S. Yoshihara, T. Aiura, and H. Noguchi, "Study on dominant mechanism of high-cycle fatigue life in 6061-T6 aluminum alloy through microanalyses of microstructurally small cracks," *Acta Mater.*, vol. 60, no. 6, pp. 2554–2567, 2012, doi: <https://doi.org/10.1016/j.actamat.2012.01.023>.
- [9] D. E. Pettit and J. M. Van Orden, "Evaluation of Temperature Effects on Crack Growth in Aluminum Sheet Material," in *Fracture Mechanics: Proceedings of the Eleventh National Symposium on Fracture Mechanics: Part I*, C. W. Smith, Ed. West Conshohocken, PA: ASTM International, 1979, pp. 106–124.
- [10] J. M. Cox, D. E. Pettit, and S. L. Langenbeck, "Effect of Temperature on the Fatigue and Fracture Properties of 7475-T761 Aluminum," in *Fatigue at Low Temperatures*, R. I. Stephens, Ed. West Conshohocken, PA: ASTM International, 1985, pp. 241–256.
- [11] P. R. Abelkis, M. B. Harmon, E. L. Hayman, T. L. Mackay, and J. Orlando, "Low Temperature and Loading Frequency Effects on Crack Growth and Fracture Toughness of 2024 and 7475 Aluminum," in *Fatigue at Low Temperatures*, R. I. Stephens, Ed. West Conshohocken, PA: ASTM International, 1985, pp. 257–273.
- [12] C. L. Walters, "The Effect of Low Temperatures on the Fatigue of High-strength Structural Grade Steels," *Procedia Mater. Sci.*, vol. 3, pp. 209–214, 2014, doi: 10.1016/j.mspro.2014.06.037.
- [13] K. S. Niaki and S. E. Vahdat, "Fatigue Scatter of 1.2542 Tool Steel after Deep Cryogenic Treatment," *Mater. Today Proc.*, vol. 2, no. 4, pp. 1210–1215, 2015, doi: <https://doi.org/10.1016/j.matpr.2015.07.033>.
- [14] H. Nazarian, M. Krol, M. Pawlyta, and S. E. Vahdat, "Effect of sub-zero treatment on fatigue strength of aluminum 2024," *Mater. Sci. Eng. A*, vol. 710, no. October 2017, pp. 38–46, 2018, doi: 10.1016/j.msea.2017.10.072.
- [15] M. P. Weiss and E. Lavi, "Fatigue of metals - What the designer needs?," *Int. J. Fatigue*, vol. 84, pp. 80–90, 2016, doi: 10.1016/j.ijfatigue.2015.11.013.
- [16] P. Gurubaran, M. Afendi, M. A. Nur Fareisha, M. S. Abdul Majid, I. Hafirman, and M. T. A. Rahman, "Fatigue life investigation of UIC 54 rail profile for high speed rail," *J. Phys. Conf. Ser.*, vol. 908, no. 1, 2017, doi: 10.1088/1742-6596/908/1/012026.
- [17] A. F. Ergenc, A. T. Ergenc, S. Kale, I. G. Sahin, V. Pestelli, and K. Dagdelen, "Reduced Weight Automotive Brake Pedal Test & Analysis," *Int. J. Automot. Sci. Technol.*, vol. 1, no. 2, pp. 8–13, 2017.
- [18] B. Riad, H. Okba, and S. Samir, "Fatigue life assessment of welded joints in a crane boom using different structural stress approaches," *J. Mech. Eng. Sci.*, vol. 13, pp. 5048–5073, 2019.
- [19] P. K. Singh, M. Gautam, and S. B. Lal, "Stress Analysis Spur Gear Design By Using Ansys Workbench," *Int. J. Mech. Eng. Robot. Res.*, vol. 5, no. 4, pp. 1560–1562, 2014.
- [20] Y. L. Fan, N. Perera, and K. Tan, "An integrated experimental and numerical method to assess the fatigue performance of recycled rail," *J. Mech. Eng. Sci.*, vol. 13, no. 4 SE-Article, Dec. 2019, doi: 10.15282/jmes.13.4.2019.18.0474.
- [21] E. M. Adigio and E. O. Nangi, "Computer Aided Design and Simulation of Radial Fatigue Test of Automobile Rim Using ANSYS," *IOSR J. Mech. Civ. Eng.*, vol. 11, no. 1, pp. 68–73, 2014, doi: 10.9790/1684-11146873.
- [22] S. R. Vempati, K. B. Raju, and K. V. Subbaiah, "Simulation of Ti-6Al-4V cruciform welded joints subjected to fatigue load using XFEM," *J. Mech. Eng. Sci.*, vol. 13, no. 3 SE-Article, Sep. 2019, doi: 10.15282/jmes.13.3.2019.11.0437.
- [23] M. F. Borges, F. V. Antunes, P. A. Prates, and R. Branco, "A numerical study of the effect of isotropic hardening parameters on mode I fatigue crack growth," *Metals (Basel)*, vol. 10, no. 2, 2020, doi: 10.3390/met10020177.

- [24] A. Carpinteri, "Crack growth resistance in non-perfect plasticity: Isotropic versus kinematic hardening," *Theor. Appl. Fract. Mech.*, vol. 4, no. 2, pp. 117–122, 1985, doi: [https://doi.org/10.1016/0167-8442\(85\)90015-1](https://doi.org/10.1016/0167-8442(85)90015-1).
- [25] R. Li *et al.*, "Advanced plasticity modeling for ultra-low-cycle-fatigue simulation of steel pipe," *Metals (Basel)*, vol. 7, no. 4, 2017, doi: 10.3390/met7040140.
- [26] Y.-L. Lee, M. E. Barkey, and H.-T. Kang, *Metal fatigue analysis handbook : practical problem-solving techniques for computer-aided engineering*. Amsterdam; London; Waltham, Mass.; Oxford: Elsevier ; Butterworth-Heinemann, 2012.
- [27] ASTM E8/E8M, "ASTM E8/E8M standard test methods for tension testing of metallic materials 1," *Annu. B. ASTM Stand.* 4, no. C, pp. 1–27, 2010, doi: 10.1520/E0008.
- [28] S. Khan, O. Kintzel, and J. Mosler, "Experimental and numerical lifetime assessment of Al 2024 sheet," *Int. J. Fatigue*, vol. 37, pp. 112–122, 2012, doi: 10.1016/j.ijfatigue.2011.09.010.
- [29] ASTM E466-15, "AMERICAN SOCIETY FOR TESTING AND MATERIALS. ASTM E466-15. Practice for conducting force controlled constant amplitude axial fatigue tests of metallic materials," *ASTM B. Stand.*, vol. i, pp. 1–6, 2015, doi: 10.1520/E0466-15.2.
- [30] R. I. Stephens, A. Fatemi, R. R. Stephens, and H. O. Fuchs, *Metal Fatigue in Engineering*. 2000.
- [31] J. Man, M. Valtr, A. Weidner, M. Petrevec, K. Obrtlk, and J. Polk, "AFM study of surface relief evolution in 316L steel fatigued at low and high temperatures," *Procedia Eng.*, vol. 2, no. 1, pp. 1625–1633, 2010, doi: 10.1016/j.proeng.2010.03.175.
- [32] S. Khan, A. Vyshnevskyy, and J. Mosler, "Low cycle lifetime assessment of Al2024 alloy," *Int. J. Fatigue*, vol. 32, no. 8, pp. 1270–1277, 2010, doi: 10.1016/j.ijfatigue.2010.01.014.
- [33] H. O. Fuchs, R. I. Stephens, and H. Saunders, *Metal Fatigue in Engineering (1980)*, vol. 103, no. 4. 1981.
- [34] F. G. L. Pereira, J. M. Lourenço, R. M. do Nascimento, and N. A. Castro, "Fracture Behavior and Fatigue Performance of Inconel 625," *Mater. Res.*, vol. 21, no. 4, 2018, doi: 10.1590/1980-5373-mr-2017-1089.
- [35] K. Tanaka and T. Mura, "A theory of fatigue crack initiation at inclusions," *Metall. Trans. A*, vol. 13, no. 1, pp. 117–123, 1982, doi: 10.1007/BF02642422.
- [36] C. Q. Bowles and J. Schijve, "The role of inclusions in fatigue crack initiation in an aluminum alloy," *Int. J. Fract.*, vol. 9, no. 2, pp. 171–179, 1973, doi: 10.1007/BF00041859.